10. Iwamoto, K.; Araki, K.; Shinkai, S. *J. Org. Chem.* **1991**, *56*, 4955.
11. Araki, K.; Iwamoto, K.; Shinkai, S.; Matsuda, T. *Chem. Lett.* **1989**, 1474.
12. Iwamoto, K.; Araki, K.; Shinkai, S. *Tetrahedron* **1991**, *47*, 4325.
13. Iwamoto, K.; Shinkai, S. *J. Org. Chem.* **1992**, *57*, 7066.
14. Groenen, L. C.; van Loon, J-D.; Verboom, W.; Harkema, S.; Casnati, A.; Ungaro, R.; Pochini, A.; Ugozzoli, F.; Reinhoudt, D. N. *J. Am. Chem. Soc.* **1991**, *113*, 2385.
15. Sheldrick, G. M. *Shelxs-86 and Shelxl-93, Program for Crystal Structure Determination*; Institute fur Anorganische Chemie der Univ., FRG, 1986.
16. *Internatioanl Table for X-ray Crystallography*; Vol IV. Kynoch Press, Birmingham, England, 1974.

Lattice Deformation and Electronic Structure of the C_{60}^+ Cation

Kee Hag Lee*, Han Myoung Lee, Hee Cha Chon, Seong Soo Park, Wang Ro Lee, T. Y. Park†, and Xin Sun§

Department of Chemistry and †Faculty of Physics, WonKwang University, Iksan 570-749, Korea
§Department of Physics, Fudan University, Shanghai 200433, China
Received January 23, 1996

The effects caused by the ionization on the electronic structure and geometry on C_{60} are studied by the modified Su-Schriffer-Heeger (SSH) model Hamiltonian. After the ionization of C_{60}, the bond structure of the singly charged C_{60} cation is deformed from I_h symmetry of the neutral C_{60} to D_{5d}, C_1, and C_2, which is dependent upon the change of the electron-phonon coupling strength. The electronic structure of the C_{60}^+ cation ground state undergoes Jahn-Teller distortion in the weak electron-phonon coupling region, while self-localized states occur in the intermediate electron-phonon region, but delocalized electronic states appear again in the strong electron-phonon region. In the realistic strength of the electron-phonon coupling in C_{60}, the bond structure of C_{60}^+ shows the layer structure of the bond distortion and a polaron-like state is formed.

Introduction

Since the recent synthesis[1] of the macroscopic quantity of the fullerene, there has been a great deal of interest in the science of fullerenes from the viewpoint of solid state[2] and molecular[3] science. Spectroscopic[4] and diffraction[5] studies have confirmed the predicted truncated icosahedral structure[6] of the C_{60} molecule. Electrochemical studies[7] have shown that C_{60} is easily reduced but is very difficult to oxidize. It should be pointed out that gas-phase reactions attributed to C_{60}^+, C_{60}^{2+}, and C_{60}^{3+} have been reported by numerous authors.[8] Kato *et al.* have isolated and studied the electronic absorption spectra of C_{60} anion and cation radicals.[9] Kukolich and Huffman have reported the EPR spectra of C_{60} anion and cation radicals.[10] There has long been the Jahn-Teller theorem, on the other hand, that molecules with high symmetry may induce structural deformations and symmetry reductions, when the highest occupied degenerate molecular orbitals (HOMOs) level is partially occupied, which provides a mechanism partly lifting this electronic degeneracy.[11] An interesting question has arisen: where will the holes of C_{60}^+ cation stay? Will they spread over the whole ball or will they be localized in some small area? If the bonds are rigid, the holes will go directly to the HOMOs, in which wave functions are extended. Otherwise, if the bonds are soft enough, the lattice can be distorted by the transferred hole to form a kind of localized state. The soliton model of Su-Schriffer-Heeger (SSH), a tight-binding model with electron-phonon (e-ph) coupling, demonstrates the novel phenomena with the midgap state in polyacetylene.[12] Several groups have studied the electronic and bond structures for the electron doped C_{60}^{n-} ($n=1$, 2, and/or 3) ground state[13~16] with the SSH model Hamiltonian. As for the C_{60}^+ cation, Harigaya[13] showed only the energy level correlation by using the SSH model Hamiltonian based on the parameters of graphite. Bendale *et al.*[17] show that a significant Jahn-Teller distortion takes place in C_{60}^+ as compared to C_{60} by using ZINDO calculations. The calculated CC bond lengths of C_{60}^+ are divided into seven classes. The CC bonds forming the pentagons and hexagons of the C_{60} structure at the top and bottom of the cage are of the same order of magnitude as in neutral C_{60}, but the twenty "equatorial" carbon atoms form CC bonds of having nearly identical bond lengths variation ($\simeq 0.01$), irrespective of whether they are part of a pentagon or a hexagon ring.

As far as we are aware, the general effect of e-ph coupling in charged C_{60}^{n-} ($n=1$, 2, 3) anions ground states is known,[14] but it is not known to the charged C_{60}^+ cation ground state. In this paper, we present the results from self-consistent numerical calculations which allow for a complete relaxation of all π electrons and individual atoms in the ground states of the C_{60}^+ cation. The different electron hopping constants

for single and double bonds are used with the SSH model Hamiltonian, which hereafter is called the modified SSH model Hamiltonian. The variation of lattice deformation is considered as a function of the ratio of the e-ph coupling constant (S) to the electron-hopping constant (T). The localized or extended character of the electronic states with the lattice deformation is also discussed. We show the calculation scheme for model Hamiltonian in section 2. The self-consistent computation, which is similar to the method proposed by Shastry,[18] and the Schmidt orthogonalization of all π orbitals in order to consider only the lattice vibration modes are used in our approach. Thus it is called the self-consistent and orthogonalized linear combination of atomic orbitals method. The merit of our model calculation lies in the speed and ease with which they yield correlation diagrams for structures of 60-atom buckminsterfullerene cation. The criterion for convergency was set to 10^{-12} for the charge iteration to ensure a highly refined structure for all calculations.

Calculation Scheme for Model Hamiltonian

As a model for the C_{60}^+ cation, we consider a buckminsterfullerene composed of 60 lattice sites and 59 electrons. The electrons move over the lattice sites by the hopping. The tight-binding approximation only considers the hopping $t_{ll'}$ between the nearest neighboring atoms sitting at r_l and $r_{l'}$, then the electron part of the Hamiltonian reads

$$H_e=-\sum_{l,l',\sigma} t_{ll'}(a_{l\sigma}{}^+ a_{l'\sigma}{}^+ + \text{h.c.} - C_{60}{}^o), \tag{1}$$

where $a_{l\sigma}{}^+$ and $a_{l'\sigma}$ are the creation and annihilation operators of electron with spin σ at sites l and l', $C_{60}{}^o$ is the bond charge between the nearest sites in the ground state of the neutral C_{60}.

The hopping coefficient $t_{ll'}$ is determined by the overlap of the wave functions of the neighboring atoms, and the overlap mainly depends on the distance between the nearest neighboring atoms. Therefore, as is commonly used in studying the charged C_{60},[13~15] the tight-binding approximation assumes that the hopping coefficient $t_{ll'}$ between the nearest sites l and l' depends only on their distance $D_{ll'}=|\vec{r}_l-\vec{r}_{l'}|$, *i.e.*

$$t_{ll'}=t(D_{ll'}). \tag{2}$$

The displacement of the atom l is

$$\vec{Q}_l=\vec{r}_l-\vec{r}_l{}^o, \tag{3}$$

where $\vec{r}_l{}^o$ is the equilibrium position of atom l in the neutral C_{60}, and the equilibrium distance between atoms l and l' is $D_{ll'}{}^o=|\vec{r}_l{}^o-\vec{r}_{l'}{}^o|$. Then the change of the distance between the nearest atoms l and l' caused by the atom displacements is

$$\begin{aligned}\Delta D_{ll'}&=D_{ll'}-D_{ll'}{}^o=|\vec{r}_l-\vec{r}_{l'}|-|\vec{r}_l{}^o-\vec{r}_{l'}{}^o|\\&=\vec{n}_{ll'}\cdot(\vec{Q}_l-\vec{Q}_{l'}),\end{aligned} \tag{4}$$

where $\vec{n}_{ll'}$ is an unit vector in the direction from site l' to site l,

$$\vec{n}_{ll'}=\frac{\vec{r}_l{}^o-\vec{r}_{l'}{}^o}{|\vec{r}_l{}^o-\vec{r}_{l'}{}^o|}. \tag{5}$$

Since the displacement $|\vec{Q}_l|$ and the distance change $\Delta D_{ll'}$ are much smaller than the distance $D_{ll'}{}^o$, the higher order terms in Eq. (4) has been neglected, and the hopping coefficient $t(D_{ll'})$ can be expanded

$$\begin{aligned}t(D_{ll'})&=t(D_{ll'}{}^o+\Delta D_{ll'})\\&=t(D_{ll'}{}^o)+S\Delta D_{ll'},\end{aligned} \tag{6}$$

where S is the derivative

$$S=\left(\frac{dt}{dD_{ll'}}\right)_{\Delta D_{ll'}=0}, \tag{7}$$

and obviously, S is a scalar.

Substituting Eq. (4) into Eq. (6), we have

$$t_{ll'}=t(D_{ll'})=t(D_{ll'}{}^o)+S\vec{n}_{ll'}\cdot(\vec{Q}_l-\vec{Q}_{l'}), \tag{8}$$

When we take the denotations

$$\vec{S}_{ll'}\equiv S\vec{n}_{ll'}, \tag{9}$$

$$T(l\text{-}l')\equiv t(D_{ll'}{}^o), \tag{10}$$

and substitute Eq. (8) into Eq. (1), H_e becomes

$$\begin{aligned}H_e=&-\sum_{l,l',\sigma} T(l\text{-}l')(a_{l\sigma}{}^+ a_{l'\sigma}+\text{h.c.})\\&-\sum_{l,l',\sigma} \vec{S}_{ll'}\cdot(\vec{Q}_l-\vec{Q}_{l'})(a_{l\sigma}{}^+ a_{l'\sigma}+\text{h.c.}-C_{60}{}^o),\end{aligned} \tag{11}$$

here, the first term is the kinetic energy and the second term the electron-phonon interaction. It should be mentioned that the interaction strength $\vec{S}_{ll'}$ between the electrons and phonons is a vector. But, from Eq. (9), it can be seen that this interaction strength $\vec{S}_{ll'}$ only depends on one coupling parameter S.

The change of distance $\Delta D_{ll'}$ yields the elastic energy E_{ela},

$$E_{ela}=\sum\frac{K}{2}(\Delta D_{ll'})^2=\sum\frac{K}{2}[\vec{n}_{ll'}\cdot(\vec{Q}_l-\vec{Q}_{l'})]^2, \tag{12}$$

where K is the elastic constant.

Then the total Hamiltonian is

$$\begin{aligned}H=&-\sum_{l,l',\sigma} T(l\text{-}l')(a_{l\sigma}{}^+ a_{l'\sigma}+\text{h.c.})\\&-\sum_{l,l',\sigma} \vec{S}_{ll'}\cdot(\vec{Q}_l-\vec{Q}_{l'})(a_l{}^+ a_{l'\sigma}+\text{h.c.}-C_{60}{}^o),\\&+\sum_{l,l'}\{P_l{}^2/2M+K/2[n_{ll'}\cdot(Q_l-Q_{l'})]^2\}\end{aligned} \tag{13}$$

where P_l is the momentum of atom l. In the adiabatic process, the kinetic energy of atoms can be neglected.

Taking $\hbar\omega_0$ as the unit of energy, we transfer all the quantities into the dimensionless form as

$$\begin{aligned}&h\equiv H/\hbar\omega_o,\ t(l\text{-}l')\equiv T(l\text{-}l')/\hbar\omega_o,\\&q_l\equiv\sqrt{(M\omega_o/\hbar)}Q_l \text{ and } s=S^2/\hbar\omega_o{}^3M_o.\end{aligned} \tag{14}$$

In terms of these dimensionless quantities, the new Hamiltonian h can be written as

$$\begin{aligned}h=&-\sum_{l,l',\sigma} t_{ll'}(m_{ll'\sigma}+m_{ll'\sigma}{}^+)\\&-\sqrt{s}\sum_{l,l',\sigma}(m_{ll'\sigma}+m_{ll'\sigma}{}^+-C_{60}{}^o)\ \vec{n}_{ll'}\cdot\vec{q}_{ll'}\\&+\frac{1}{2}\sum(\vec{n}_{ll'}\cdot\vec{q}_{ll'})^2\end{aligned} \tag{15}$$

where $m_{ll'\sigma}=a_{l\sigma}{}^+ a_{l's}$, $t_{ll'}=t(l\text{-}l')$ and $\vec{q}_{ll'}=\vec{q}_l-\vec{q}_{l'}$.

Hereafter we calculated the adiabatic potential $\varepsilon(\{\vec{q}_{ll'}\})$ of

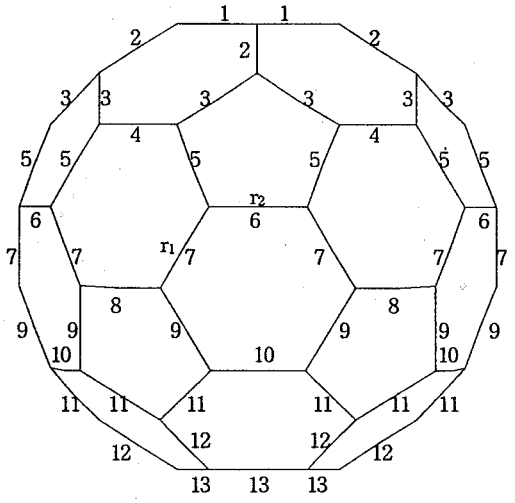

Figure 1. The layer structure of bonds of the 60-atom carbon cluster buckminsterfullerene structure. This structure has 60 vertices, 20 hexagonal faces, and 12 pentagonal faces. Each carbon atom occupies each vertex. There are two topologically different bond lengths: the length (r_1) separating hexagons and the length (r_2) separating a hexagon from a pentagon.

the lowest energy eigenstate, $|G>$, of Eq. (15) for eigenvalues of deformation $\{\vec{q}_{ll'}\}$ and minimized ε with respect to the whole set $\{\vec{q}_{ll'}\}$.

Since the self-consistent values of $\{\vec{q}_{ll'}\}$ for the C_{60}^+ cation may be entirely different from those for neutral C_{60}, graphite, and diamond, our reformulation is based on a principle where both $\{\vec{q}_{ll'}\}$ and the set of eigenfunctions, $\{\Psi_l\}$, are treated as variables. We apply the Schmidt orthogonalization to obtain orthonormality and completeness relations for the amplitudes, and apply the Feynman-Hellman theorem with the Lagrange multiplier for the extreme points. We described the above process in detail at ref. [14].

In practical calculations, we assume that $T(l\text{-}l')$ between nearest neighbor sites in 30 bonds (r_1) which lie solely in the six-membered ring (6-MR), is T, while that in 60 bonds (r_2) which form the edges of both a five-membered ring (5-MR) and a 6-MR, is 0.9T (see Figure 1).

Eq. (15) is solved by self-consistent iteration. As mentioned before, we are interested mainly in a general case of e-ph interaction in the C_{60}^+ cation ground states in which the value of s/t ranges from 0.0 to 2.0.

Results and Discussion

In our Hamiltonian, we do not include the explicit Coulomb interactions between π electrons, which is similar to the standard arguments given in the previous papers.[13~15,19]

In the ground state for the C_{60}^+ cation, the degenerate HOMOs of the neutral C_{60} ground state are partially filled. As is well known this kind of ionic system relaxes to the lattice configuration with reduced symmetry. The self-consistent solution is obtained from Eq. (15), which has 11 different s/t values from 0.0 to 2.0. Total energies, number of localization (NL), and number of bond charge difference (NBCD) for the C_{60}^+ cation ground state are shown in Figure 2.

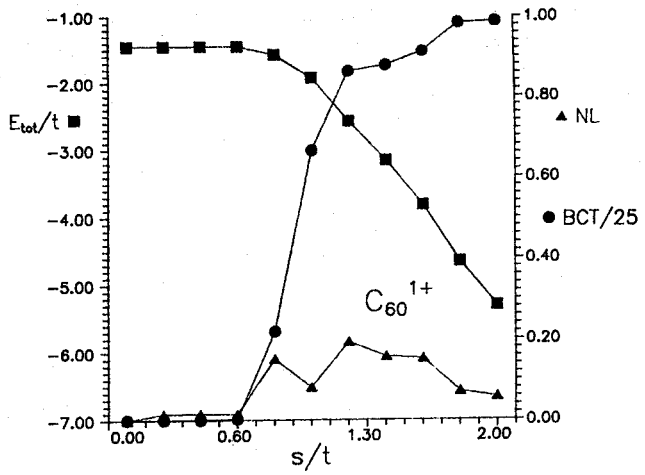

Figure 2. Total energies, the number of localization (NL), and the number of bond charge difference (NBCD) in the C_{60}^+ cation ground state.

Here, NL defined as

$$NL=\{\int(|\phi_L|^2-|\phi_T|^2)d\tau\}^2 = \sum_L (S_L-S_T)^2 \quad (16)$$

was calculated for each unique s/t. In Eq. (16), L is a site, and S_L and S_T is a localized charge density at site L with and without the electron-phonon coupling constant, respectively. Here the MOs were orthogonalized by the Schmidt method.

NBCD defined as

$$NBCD=\sum_{(i,j)=k}\{(BC)_k-(BCC_{60})_k\}^2 \quad (17)$$

was calculated for each unique s/t, where BC is the bond charge between nearest neighbor i-site and j-site in the C_{60}^+ cation ground states and BCC_{60} is the same bond charge in the neutral C_{60} ground states.

As shown in Figure 2, the self-consistent solution in this case is that there are three regions based on e-ph coupling strength with small, intermediate, and large values of the e-ph coupling constant, respectively. The shapes of NL, NBCD and E_{tot}/t are similar to those of ionic C_{60}^{n-} ($n=1$, 2, 3) anions ground states, but NL of the C_{60}^+ cation ground states in the weak electron-phonon region is larger than those of C_{60}^{n-} ($n=1$, 2, 3) anions. It means that the electronic state of the C_{60}^+ cation ground states is more localized than those of the C_{60}^{n-} ($n=1$, 2, 3) anions ground states in the region of Jahn-Teller distortion. The s/t value which has the maximum NL is 1.2 for the C_{60}^+ cation ground state. When we pass the maximum NL value the states become again delocalized. The larger s/t value has the larger NBCD in the C_{60}^+ cation ground state. The s/t value which has the maximum NL value in the C_{60}^+ cation ground state has the maximum slope variation between nearest neighbor NBCDs. After we pass this specific value, the NBCD is almost unchanged like those of C_{60}^{n-} ($n=1$, 2, 3).

From the self-consistent calculation, we obtain D_{5d}, C_1, and C_2 symmetries of deformed lattices for the C_{60}^+ cation ground states as a function of s/t and show their features

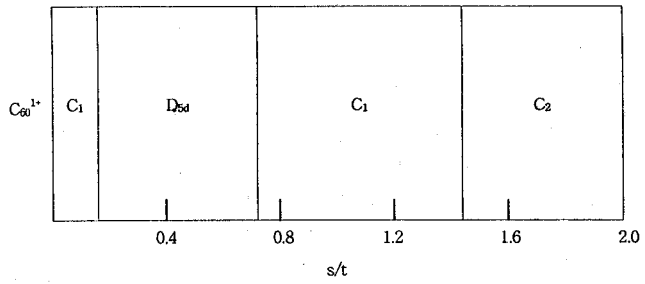

Figure 3. Deformation lattices as a function of s/t values in the C_{60}^+ cation ground state.

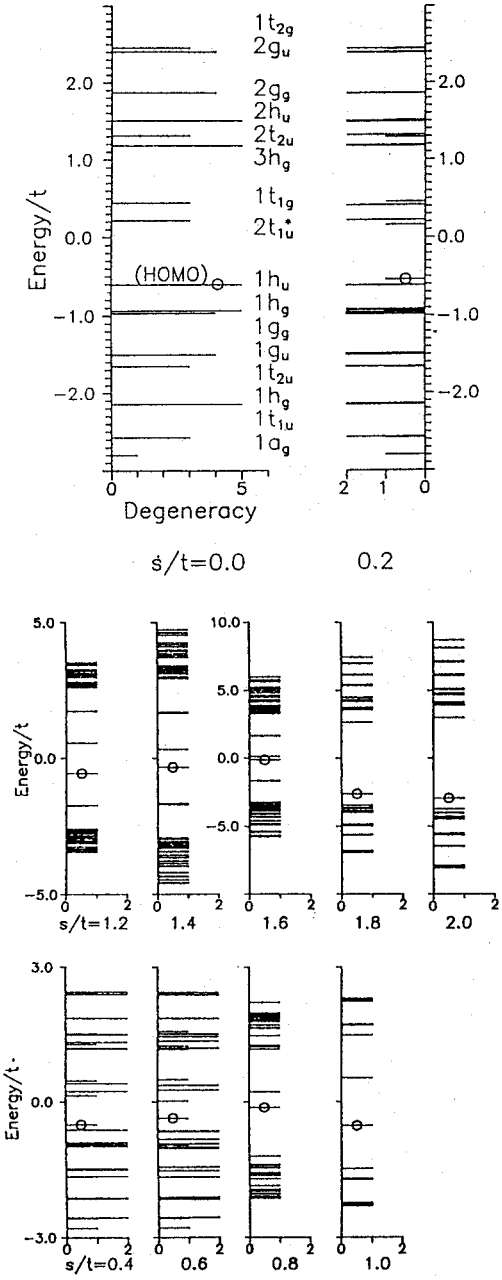

Figure 4. Energy levels and the degeneracies measured by the length of each parallel bar of the eigenenergies $\{E_i/t\}$ in the relaxed geometry of each ground state related to specific s/t values.

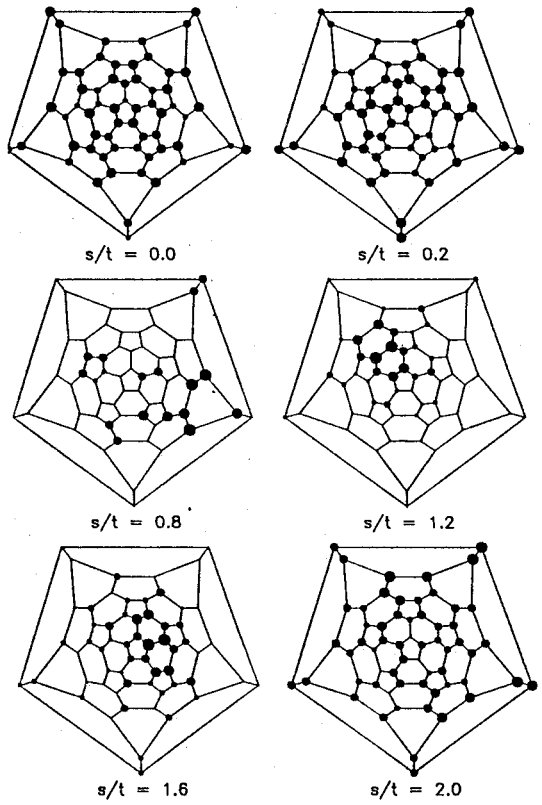

Figure 5. Schlegel diagrams for the electron density distribution on C_{60}^+ ground states with specific s/t values.

in Figure 3. The energy levels and their degeneracies for each case of relaxed geometries in the C_{60}^+ cation ground state are shown in Figure 4. As shown in Figure 4, there are 11 panels for 11 different values of s/t from 0.0 to 2.0. In each panel the position of each parallel bar marks the value of one eigenenergy and the height of the bar measures the corresponding degeneracy. The widths of two eigenenergies at the ends of each energy spectrum as a function of s/t in the C_{60}^+ cation ground state are divided approximately into three regions as follows: an approximately constant region up to less than 0.8 for s/t; a small decreased region with from 0.8 to less than 1.4 for s/t; a large increased region with 1.4-2.0 for s/t.

In the region of s/t less than 0.8 in the C_{60}^+ ground states, the e-ph coupling is a perturbation to the electron-hopping and elastic energy terms, which is the physical origin of the Jahn-Teller effect. In the regions, total energy is linearly dependent upon the s/t values, and the slope is very small like those of charged C_{60}^{n-} ($n=1$, 2, 3) anions.

In the triple degenerate states, the splitting of the degeneracy agrees with the analytical solution obtained from the application of first order degenerate perturbation theory. That the t_{1u} level splits, as indicated in Figure 4 for example, agrees with the analytical solution ($-2v$ and v for a_{2u} and e_{1u} levels, respectively) by applying the first order degenerate perturbation theory to the t_{1u} degenerate states (see ref. [14]). As shown in Figure 5, this leads to a distortion which has a reduced D_{5d} symmetry, picking out a radial direction through the center of a pentagon. The splitting of the t_{1u} level by the e-ph coupling in this region of the C_{60}^+ cation

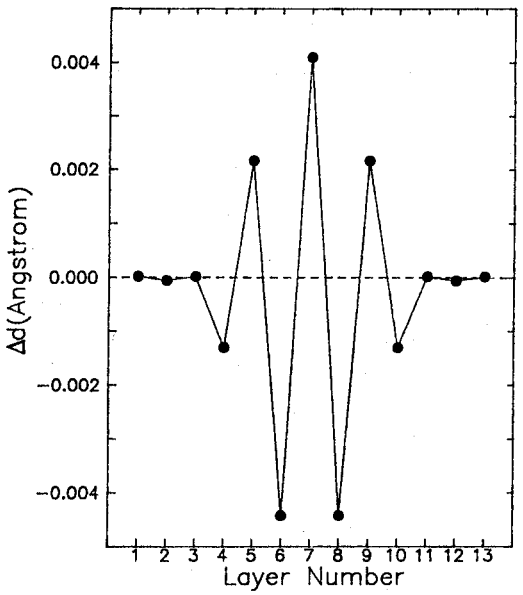

Figure 6. The layer-dependence of bond-length changes Δd in C_{60} by an electron ionization.

ground states matches the results of Lee *et al.*,[14] Varma *et al.*[20] and Schluter *et al.*,[21] which is based on the Jahn-Teller distortion. But in the regions of intermediate and strong e-ph coupling, each degenerate level splits in nondegenerate levels, and the deformed lattices may give rise to localized electronic states. In the region where the e-ph coupling is strong, the total energy is linearly dependent upon the s/t values with much larger coefficient of linearity.

The electron density distribution on the C_{60}^+ cation ground states as shown in Figure 5 is used to represent deformed lattices. For illustrative purpose here, we use a Schlegel diagram (two dimensional representation) of the three-dimensional system as shown in Figure 5. In the C_{60}^+ cation ground state with s/t values less than 0.8, the deformed lattices (see Figure 5) have the reduced D_{5d} symmetry (but not among the crystallographic group) which has a fivefold rotation (and a tenfold improper rotation axis), five twofold rotation axis (and five σ_d symmetry planes), and inversion center.

Here the four- and fivefold degenerate states, which are in the vector representation of the icosahedral group (I_h), split into 2+2 and 2+2+1 states, respectively, as the threefold degenerate states split into onefold and twofold states. Here, the T_{1u} state for the LUMOs in C_{60} splits into A_{2u} and E_{1u} states in C_{60}^+, and the H_u state for the HOMOs in C_{60} into A_{1u}, E_{1u} and E_{2u} states in C_{60}^+ as shown in Figure 4. While the deformed lattices in the intermediate e-ph coupling region give rise to localized electronic states, the deformed lattices in the strong e-ph coupling region reproduce the delocalized electronic states. The geometrical structure of the C_{60}^+ cation ground state reduces from I_h to D_{5d}, C_1 and C_2 due to the relative strength of e-ph coupling constant to electron-hopping constant.

In order to demonstrate the lattice distortion distinctly the truncated icosahedron of C_{60} is oriented in such a way that the top and bottom faces are the pentagons, which are shown in Figure 1, then all 90 bonds in C_{60} are divided into 13 layers indicated by the numbers in Figure 1. Before an electron ionization, there are only two kinds of bond in the neutral C_{60}: the double bonds (r_1) in the border between two 6-MRs, and the single bonds in the border between 5-MR and 6-MR. The former is a short bond with length r_1= 1.402 and the latter is a long bond with length r_2=1.435 in ref. [14]. The layers with numbers 2, 4, 7, 10, 12 are double bonds, and the rest are single bonds.

In order to estimate the electron-phonon effect for the real C_{60} molecule by an electron ionization, we choose the realistic parameters used in ref. [22], and the electron-phonon coupling dimensionless parameter (λ=s/t=0.198≒0.2). After an electron ionization the lattice structure is distorted and the bond lengths change. The bonds in the same layer get same changes in their bond lengths, but the change Δd of the bond length depends on the layer. In the case of D_{5d} the layer-dependence of the changes Δd is shown in Figure 6. It can be seen from Figure 6 that the distortion mainly takes place in the equator area (6, 7, 8-th layers). Other layers have only little distortion. Such localized distortion is called as "string polaron" like the electron uptake case[13~15] of C_{60}. But the absolute magnitude of distortion of each layer in C_{60}^+ cation is less than that in C_{60}^- anion. The change of the bond lengths in 2-, 4-, 10-, and 12-th layers of C_{60}^+ cation has the opposite distortion (*i.e.*, $\Delta d<0$) compared to that in C_{60}^- anion. Our results show the same ground state structure (D_{5d} symmetry) and layer-dependence of bond length changes Δd as the ZINDO results. Since the results given in the ZINDO calculation are the total effect produced by both electron-phonon and electron-electron interactions, our results show that the D_{5d} layer structure of bond distortion of C_{60}^+ is mainly produced by the electron-phonon coupling.

Acknowledgment. This work was supported by a research grant from the WonKwang University (1995), the Basic Science Research Institute Program, Ministry of Education (BSRI-95-3438), and the KOSEF (94-0501-11-3) of Korea, and by the National Science Foundation of China.

References

1. Krotschmer, W.; Lamb, L. D.; Fostiropoulos, K.; Huffman, D. R. *Nature* **1990**, *347*, 354.
2. Diederich, F.; Whetten, R. L. *Acc. Chem. Res.* **1992**, *25*, 119.
3. Olah, G. A.; Bucsi, I.; Aniszfeld, R.; Prakash, G. K. S. *Carbon* **1992**, *30*, 1203.
4. Yanoni, C. S.; Bernier, P. P.; Bethune, D. S.; Meijer, G.; Salem, J. R. *J. Am. Chem. Soc.* **1991**, *113*, 3190.
5. Hawkins, J. M.; Meyer, A.; Lewis, T. A.; Loren, S.; Hollander, H. F. *Science* **1991**, *252*, 312.
6. Kroto, H. W.; Heath, J. R.; O'Brien, S. C.; Curl, R. F.; Smally, R. E. *Nature* (London) **1985**, *318*, 162.
7. Dubois, D.; Kadish, K. M.; Flanagan, S.; Haufler, R. E.; Chibante, L. P. F.; Wilson, L. J. *J. Am. Chem. Soc.* **1991**, *113*, 7773.
8. Javahery, G.; Petrie, S.; Wincel, H.; Wang, J.; Bohme, D. K. *J. Am. Chem. Soc.* **1993**, *115*, 5716 and references therein.

9. Kato, T.; Kodama, T.; Nakagawa, T.; Matsui, Y.; Suzuki, S.; Shiromaru, H. *Chem. Phys. Lett.* **1991**, *180*, 446.
10. Kukolich, S. G.; Huffman, D. R. *Chem. Phys. Lett.* **1991**, *182*, 263.
11. Liehr, A. D. *Ann. Rev. Phys. Chem.* **1962**, *13*, 47.
12. Su, W. P.; Schriffer, J. R.; Heeger, A. *Phys. Rev.* **1983**, *B22*, 2099; *ibid,* **1983**, *B28*, 1138; *Phys. Rev. Lett.* **1979**, *42*, 1698.
13. Harigaya, K. *Phys. Rev.* **1992**, *B45*, 13676. Friedman, B. *Phys. Rev.* **1992**, *B45*, 1454. Fu, R. T.; Sun, X.; Chen, Z. *Chinese Phys. Lett.* **1992**, *9*, 541.
14. Lee, K. H.; Paek, U. *J. Phys. Chem. Solids* **1993**, *54*, 565.
15. Fu, R. T.; Lee, K. H.; Park, T. Y.; Sun, X.; Yu, Z. G. *Bull. Korean Chem. Soc.* **1994**, *15*, 112.
16. Fu, R. T.; Fu, R.; Lee, K. H.; Sun, X.; Ye, H. J.; Yu, Z. G. *Bull. Korean Chem. Soc.* **1993**, *14*, 740.
17. Bendale, R. D.; Stanton, J. F.; Zener, M. *Chem. Phys. Lett.* **1992**, *194*, 467.
18. Shastry, B. S. *J. Phys.* **1983**, *A16*, 2049.
19. Friedman, B.; Harigaya, K. *Phys. Rev.* **1993**, *B47*, 6975.
20. Varma, C. M.; Zaanen, J.; Raghavachari, K. *Science* **1991**, *254*, 989.
21. Schluter, M.; Lannoo, M.; Needels, M.; Baraff, G. A.; Tomanek, D. *Phys. Rev. Lett.* **1992**, *68*, 526.
22. You, W. M.; Wang, C. L.; Zhang, F. C.; Su, Z. B. *Phys. Rev.* **1993**, *B47*, 4765.

Solid-State ^{31}P NMR Chemical Shielding Tensors in Binuclear Platinum Diphosphite Complexes

Ae Ja Woo* and Leslie G. Butler

**Department of Science Education, Ewha Womans University, Seoul 120-750, Korea*
Department of Chemistry, Louisiana State University, Baton Rouge, Louisiana 70803, U.S.A.
Received February 1, 1996

The principal elements of the ^{31}P NMR chemical shielding tensors have been determined for three binuclear platinum diphosphite complexes, $K_4[Pt_2(P_2O_5H_2)_4]\cdot 2H_2O$ ("Pt_2"), $K_4[Pt_2(P_2O_5H_2)_4Cl_2]\cdot 2H_2O$ ("Pt_2Cl_2"), and $K_4[Pt_2(P_2O_5H_2)_4Br_2]\cdot 2H_2O$ ("Pt_2Br_2"), by using a Herzfeld-Berger graphical method for interpreting the ^{31}P MAS spectrum. The orientations of ^{31}P chemical shielding tensor relative to the molecular axis system are partially assigned with combination of the longitudinal relaxation study of HPO_3^{2-} and the reference to known tensor orientations of related sites; the most chemical shielding component, δ_{33}, is directed along the P-Pt bond axis. A discussion is given in which the experimental principal elements of the ^{31}P chemical shielding tensor are related with the Pt-Pt bond distances in binuclear platinum diphosphite complexes.

Introduction

Solid-state NMR spectroscopy of S=1/2 nuclei, principally ^{13}C and ^{31}P, has been utilized to yield information concerning the molecular geometry, electronic structure, and motion of molecules in organometallic systems. ^{31}P NMR spectroscopy has been more frequently used than ^{13}C in the organometallic studies, because of the 100% natural abundance and the relatively high sensitivity of the ^{31}P nucleus. ^{31}P chemical shielding tensors have been successfully correlated with the molecular structural parameters such as bond angles and bond distances in phosphido-bridged complexes and phosphates.[1,2] Similarly, the correlation between the ^{31}P isotropic chemical shift and the cation charge of orthophosphates has been investigated.[3] The *cis-trans* isomerization of $(R_3P)_2MCl_2$ (M=Pd, Pt)[4,5] and the determination of NMR parameters in cyclic/acyclic phosphine complexes[6,7] have been studied by ^{31}P CP/MAS NMR spectroscopy. In addition, the effects of molecular motion for solid P_4[8] and phase transition for P_4S_3[9] on ^{31}P NMR spectra have been investigated. Two-dimensional ^{31}P CP/MAS NMR techniques have been applied to separate the unresolved interactions in the metal phosphine complexes.[10]

Binuclear platinum diphosphite complexes, $K_4[Pt_2(P_2O_5H_2)_4]\cdot 2H_2O$ ("Pt_2"), $K_4[Pt_2(P_2O_5H_2)_4X]\cdot 2H_2O$ ("Pt_2X"), and $K_4[Pt_2(P_2O_5H_2)_4X_2]\cdot 2H_2O$ ("Pt_2X_2"; X=Cl, Br, I), have attracted attention because they can be used to prepare linear chain structures with the electrical properties of a semiconductor.[11~15] The semiconductivity of these complexes have been indirectly investigated by the determination of the intermetallic bond distances from X-ray crystallography. The intermetallic bonding have also been characterized from electronic and vibrational spectroscopic data.[16~18] Herein, three principal elements and the partial orientation of the ^{31}P chemical shielding tensors for Pt_2, Pt_2Cl_2, and Pt_2Br_2 were determined by using the solid-state ^{31}P MAS spectroscopy. Consequently, the NMR results will be related to the Pt-Pt distances in the molecular structures, Pt_2 and Pt_2X_2, to access information about the changes in the Pt-Pt bond that are so important to conduction in the Pt_2X system.

*To whom correspondence should be addressed.